



## Editor's Choice

## Structural origin for electron affinity of phenanthrene and ion cores of phenanthrene anion clusters

Sang Hak Lee<sup>a</sup>, Jae Kyu Song<sup>b,\*</sup>, Seong Keun Kim<sup>a,\*</sup><sup>a</sup> Department of Chemistry, Seoul National University, Seoul 151-747, Republic of Korea<sup>b</sup> Department of Chemistry, Kyung Hee University, Seoul 130-701, Republic of Korea

## ARTICLE INFO

## Article history:

Received 21 February 2015

In final form 12 March 2015

Available online 20 March 2015

## ABSTRACT

We studied anion clusters of phenanthrene using photoelectron spectra and theoretical calculations. The electron affinity of phenanthrene, which lies between those of naphthalene and anthracene, was explained by the orbital interaction model that reflected the structural differences among these molecules. The spectral feature of the photoelectron spectra indicated strong electron-vibration coupling along two symmetric vibrational modes. Since the spectral features of each ion core structure were uniquely characteristic, we could identify that the pentamer anion had coexisting monomeric and trimeric cores on the basis of the shape of the photoelectron spectra and the size-dependent evolution of the electron affinity.

© 2015 Elsevier B.V. All rights reserved.

## 1. Introduction

Binding of an electron to a molecular system is of primary importance in many areas [1–3]. The anion is formed upon the occupation of a low-energy empty molecular orbital by an excess electron [4–13], where the electron affinity (EA) represents the relative stability of the anion compared to its neutral counterpart. Since EA is correlated with the molecular orbital energy levels, EAs of the polycyclic aromatic hydrocarbon (PAH) molecules generally increase with increasing molecular size: benzene (−1.12 eV) [5], naphthalene (−0.19 eV) [5], anthracene (0.54 eV) [8,9], and tetracene (1.05 eV) [10]. However, EAs of other PAHs are not explained simply by the molecular size, as in phenanthrene (0.12 eV) and pyrene (0.45 eV) [11–13]. These molecules have “non-linear” structures unlike the conforming series above and possess EAs significantly smaller than those of equal-sized molecules. In this regard, phenanthrene affords a clue to unravel the correlation between the geometric and electronic structures of the anionic valence state [14], which may shed light on why its EA is so different from the EA of anthracene despite their identical chemical formula and size.

The spectral features of the photoelectron spectrum often reveal the nature of the ion core in the cluster system [15–18], as the size-dependent evolution of EAs is also indicative of the ion core present in the clusters [10,11]. For instance, the photoelectron spectral

shape of naphthalene dimer anion suggests that it consists of a monomeric ion core and a single neutral solvent, rather than a dimeric ion core [18]. In another example, the existence of multiple ion cores was deduced from the spectral evolution of the anion clusters of anthracene and phenanthrene [9,13].

In this study, we present the photoelectron spectra and theoretical calculations of phenanthrene anion clusters. The EA of phenanthrene was consistent with the chemical trend for the  $\pi$  orbital system expansion, which was explained by the structural component model for the PAH system. The photoelectron spectrum also indicated that the vibrational progression of the symmetric modes was strongly affected by the ion-induced intermolecular interactions. A multiple ion core model involving the monomeric and trimeric ion cores was proposed for the pentamer anion of phenanthrene.

## 2. Experimental

The experimental setup is only briefly described because the details of the anion mass spectrometer and the photoelectron spectrometer have been previously reported [13,15]. The pulsed molecular beam was generated by expanding phenanthrene vapor (160 °C), which was seeded in Ar carrier gas with a stagnation pressure of  $\sim 7$  atm. The molecular beam was intersected by an electron beam (400 eV, 300  $\mu$ A) to produce anion clusters using slow secondary electrons. The anion clusters traveled in a Wiley-McLaren-type 1.8 m time-of-flight mass spectrometer, where the resolution of the mass spectrometer ( $M/\Delta M$ ) was about 200. A mass

\* Corresponding authors.

E-mail addresses: [jaeksong@khu.ac.kr](mailto:jaeksong@khu.ac.kr) (J.K. Song), [seongkim@snu.ac.kr](mailto:seongkim@snu.ac.kr) (S.K. Kim).

distribution of phenanthrene cluster anions indicated the appearance of the monomer anion,  $\text{Pn}_1^-$ , and single solvents ( $\text{H}_2\text{O}$  and Ar) stabilized the monomer anion effectively [13]. The anions of interest selected by a mass gate were allowed to enter the photoelectron spectrometer. The kinetic energies of the selected anions were decelerated to less than 20 eV by a potential switch in order to reduce Doppler broadening in the photoelectron spectra. The photoelectron spectra were obtained at 1064 and 740 nm using an Nd:YAG laser and a dye laser, respectively. The full width at half maximum energy resolution of the magnetic-bottle-type photoelectron spectrometer was about 0.05 eV at 1 eV electron kinetic energy.

### 3. Results and discussion

#### 3.1. Orbital interaction in phenanthrene

The EA of  $\text{Pn}_1^-$  was reported as 0.12 eV [13], where the partially resolved spectral characteristic in the photoelectron spectrum was attributed to the symmetric vibrational mode of neutral phenanthrene ( $A_1$ , 0.181 eV,  $1458\text{ cm}^{-1}$ , mode 1) [14,19]. However, the inclusion of another symmetric vibrational mode ( $A_1$ , 0.132 eV,  $1068\text{ cm}^{-1}$ , mode 2) reproduced a more appropriate photoelectron spectrum (Figure 1a) than did the single progression of mode 1 (Figure S1). The observed vibrational progression of modes 1 and 2 indicated that the stable geometry of the anion was different from that of the neutral structure, mainly along the C–H wagging modes (Figure 1b), because the electron–vibration coupling of modes 1 and 2 was strong in  $\text{Pn}_1^-$  [14]. In this regard, the deconvolution results supported the previous study [13], which suggested that vertical

detachment energy (VDE) was the 0–0 transition energy of  $\text{Pn}_1^-$ , i.e., EA of phenanthrene.

Generally, an excess electron is not accommodated in small planar aromatic hydrocarbons, so that the smallest one (benzene) has a negative EA ( $-1.12\text{ eV}$ ) [5]. However, the EAs of PAH molecules increase with increasing number of  $\pi$  electrons, because the expansion of  $\pi$  orbital systems leads to delocalization of an excess electron over the molecular framework. Thus the EAs of naphthalene, anthracene, and tetracene are  $-0.19$ ,  $0.54$ , and  $1.05\text{ eV}$  [5,8–10], respectively, which supports that the increasing number of  $\pi$  electrons renders the electron attachment less prohibitive through delocalization. On the other hand, the EA of phenanthrene ( $0.12\text{ eV}$ ) is much smaller than that of anthracene ( $0.54\text{ eV}$ ), despite their identical molecular formula ( $\text{C}_{14}\text{H}_{10}$ ), which implies that the number of  $\pi$  electrons in PAH molecules is not the sole reason for the increase of EA. Phenanthrene provides a clue to the correlation between EA and the molecular framework, because both phenanthrene and anthracene can be partitioned to naphthalene and butadiene moieties. However, the molecular orbital energy levels, such as the highest occupied molecular orbital (HOMO) and the lowest unoccupied molecular orbital (LUMO), are suggested to be different in the previous study [14], due to the characteristic reaction position of the butadiene moiety with respect to naphthalene (Figure 2a). For anthracene, the HOMO of naphthalene interacts strongly with that of butadiene due to the good match of orbital symmetries (Figure S2), so that the in-phase combination stabilizes HOMO-1 and the out-of-phase counterpart pushes up the HOMO of anthracene (Figure 2b). The LUMOs of naphthalene and butadiene also interact effectively, which stabilizes the LUMO of anthracene by the in-phase combination, so that the energy difference between HOMO and LUMO of anthracene is smaller than that of naphthalene. In the case of phenanthrene, however, the HOMOs of naphthalene and butadiene are suggested to have only a weak interaction at the connecting sites due to the mismatch of orbital symmetries (Figure S2) in the previous study [14]. In addition, the LUMOs of naphthalene and butadiene have little interaction. The LUMO of naphthalene can interact with the HOMO of butadiene to some extent, which stabilizes the orbital energies in phenanthrene by electron delocalization.

Indeed, this orbital interaction model agreed with our calculation results. For example, the calculated shape of the LUMO of phenanthrene, which became the singly occupied molecular orbital (SOMO) of the phenanthrene anion, matched the shape in the orbital interaction model. Accordingly, the shape of SOMO explained the spectral feature of the photoelectron spectrum (Figure 1a), where the vibrational progression of mode 1 was more prominent than that of mode 2. In other words, the asymmetric vibrational motions along the nodes in SOMO were more found in mode 1 than mode 2 (Figure 1b), so that the occupation of SOMO seemed to perturb the molecular coordinates of mode 1 more strongly. Therefore, the effect of the excess electron appeared mainly in mode 1, which enlarged the Franck–Condon factors of mode 1.

The orbital interaction model also explained the decrease in the ionization energy (IE) from  $8.15$  to  $7.86$  and  $7.41\text{ eV}$  [20], with the expansion of the  $\pi$  orbital systems from naphthalene to phenanthrene and anthracene, respectively (Figure 2c). Indeed, the HOMO of phenanthrene was less pushed up than that of anthracene, because the energy of HOMO was correlated to IE according to Koopmans' theorem [21]. The energy difference between HOMO and LUMO ( $S_0$ – $S_1$  transition energy), which decreased from  $3.97\text{ eV}$  for naphthalene to  $3.63$  and  $3.43\text{ eV}$  for phenanthrene and anthracene, respectively [22–24], also presented a similar propensity. The  $S_0$ – $S_1$  transition energy of phenanthrene was larger than that of anthracene, because the LUMO of phenanthrene was less stabilized than that of anthracene. Likewise, the small EA

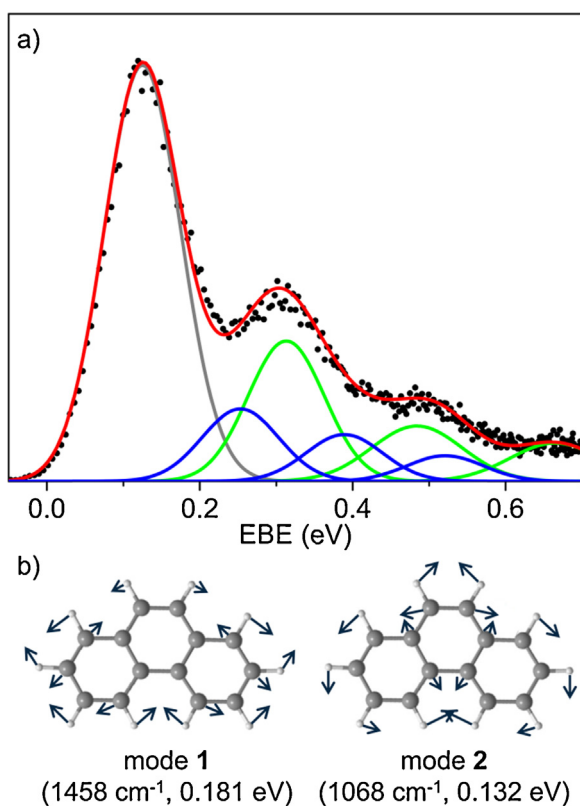


**Figure 1.** (a) Photoelectron spectrum of the phenanthrene monomer anion,  $\text{Pn}_1^-$ , is deconvoluted by vibrational progression of mode 1 (green line) and mode 2 (blue line). The gray line indicates the 0–0 transition. (Modified from Ref. [13]). (b) The vibrational motions of the totally symmetric C–H wagging modes (modes 1 and 2) are schematically represented. (For interpretation of the references to colour in this figure legend, the reader is referred to the web version of this article.)

Download English Version:

<https://daneshyari.com/en/article/5380008>

Download Persian Version:

<https://daneshyari.com/article/5380008>

[Daneshyari.com](https://daneshyari.com)